Thermodynamics of the QCD_{1+1} nonrelativistic baryon gas

Michael Engelhardt
Department of Condensed Matter Physics, Weizmann Institute of Science, Rehovot 76100, Israel
(Received 23 June 1994)

The nonrelativistic baryon gas of QCD_{1+1} for SU(2) color is studied in the low density regime using two complementary approaches: In the classical limit, the Gibbs free energy can be evaluated analytically, yielding an exact value for the second virial coefficient and a bound for the equation of state at higher densities. Certain thermodynamic observables can already be given for the entire range of densities due to simple scaling properties. On the other hand, a quantum mechanical baryon-baryon scattering calculation yields the behavior of the second virial coefficient away from the classical limit down to low temperatures.

PACS number(s): 12.38.−t, 12.39.Hg, 24.85.+p

I. INTRODUCTION

One of the fundamental issues of modern-day strong interaction physics is the description of hadronic matter in terms of quark degrees of freedom. Since there is no clear separation between the length scales governing hadron substructure and the ones entering hadron-hadron interactions, there is no *a priori* reason why a description of hadronic systems based on hadron constituents should be a good approximation to QCD dynamics. In fact, the great difficulties encountered to date with respect to identifying unambiguous signals of quark substructure in the studies of heavy ion collisions come rather as a surprise. Despite confinement, it is thus important to consider multiple-quark systems beyond the description of single hadrons. Indeed, one expects the hadronic picture to completely break down at sufficiently high densities or temperatures; here, a quark-gluon plasma [1] with virtually freely propagating quarks is thought to form, since, in the language of the nonrelativistic quark model, the quarks need little energy to jump from one linearly confining potential well to another. Because the energy densities necessary for the production of a quark-gluon plasma and/or for probing the quark substructure of many-hadron systems are expected to be accessible experimentally, especially with the advent of high-energy accelerators such as RHIC and LHC, considerable attention has been devoted in recent years to the study of the transition between the hadronic and quark phases.

Whereas it is possible to argue that, in the high-density, high-temperature regime, asymptotic freedom allows the use of perturbative methods to treat the quark-gluon dynamics, at low energies, especially in the conventional hadronized regime, a nonperturbative treatment becomes unavoidable. In contrast to the properties of single hadrons, which can be calculated reasonably well using some phenomenological assumptions (e.g., the nonrelativistic quark model or the MIT bag model), the multihadron problem has proven to be considerably more difficult, regardless of whether one considers a few-hadron system (e.g., hadron-hadron scattering) or extended nuclear matter (e.g., the equation of state in a neutron star).

Among other approaches, the nonrelativistic quark-exchange model [2] has figured prominently in these studies. Motivated by a flux-tube picture, it constitutes a many-body interaction on the quark level which, by construction, avoids the long-range van der Waals forces between hadrons inherent in any superposition of two-body forces [3]. Meson-meson scattering in this framework has been treated, e.g., in [2], [4], and [5]; extended nuclear matter was considered using a thermodynamic Green's function approach, taking account of nearest-neighbor Pauli blocking, in [6–8]. Further extended matter calculations employing Monte Carlo methods were performed in [9–12]. These latter calculations have up to now focused on the ground state of a one-dimensional system of quarks as a function of density.

In this simpler one-dimensional setting, it is indeed possible to show that the quark exchange model is an exact consequence of QCD_{1+1} for heavy, nonrelativistic quarks [13]. Thus, in this case, the gap between the underlying field theory and tractable models has been bridged and a quark-exchange model calculation in fact represents an exact evaluation of QCD_{1+1} properties for nonrelativistic quarks. The motivation of the present work, which focuses on the equation of state of the QCD_{1+1} baryon gas with SU(2) color, is thus twofold: On the one hand, it complements the ongoing Monte Carlo investigations of the ground state mentioned above; on the other hand, it represents a study of the many-body properties of QCD_{1+1} itself, deriving observables in the hadronized phase directly from the underlying field theory, albeit in the simple one-dimensional nonrelativistic case.

Specifically, this work treats the baryon gas on two levels: On the one hand, the system is studied in the classical limit, where the partition function can be evaluated analytically in the low-density regime, yielding an exact result for the second virial coefficient and a bound for the complete equation of state. On the other hand, an exact quantum mechanical calculation of the S matrix for baryon-baryon scattering is performed, yielding the second virial coefficient of the baryon gas also in the low-temperature regime.

II. REVIEW OF QCD_{1+1} WITH NONRELATIVISTIC QUARKS

The physics of QCD_{1+1} with nonrelativistic quarks and SU(2) color can be summarized as follows [13]: The color degrees of freedom evolve (in the infinite volume limit) on an infinitely faster time scale than the positions of the quarks. Thus, an adiabatic treatment in the spirit of the Born-Oppenheimer approximation is exact. Solving the Schrödinger equation for the color degrees of freedom while the quark positions are fixed yields the result that the colors of the quarks must be coupled to an overall singlet, and it yields the effective potential governing the position space dynamics of such configurations. Thus, there is only one possible color configuration for two quarks (here, $\psi^\dagger$ denotes a quark creation operator),

$$|\phi_2\rangle = \frac{1}{\sqrt{2}}[\psi_1^\dagger(x_1)\psi_2^\dagger(x_2) - \psi_2^\dagger(x_1)\psi_1^\dagger(x_2)]|0\rangle = \frac{1}{\sqrt{2}}(|12\rangle - |21\rangle), \tag{1}$$

and the potential energy associated with this state is[1]

$$V|\phi_2\rangle = \frac{3}{8}g^2|x_1 - x_2|\,|\phi_2\rangle. \tag{2}$$

In the case of four quarks, one has two possible ways of coupling the quarks to overall color singlets, namely [in obvious notation; cf. (1)],

$$|\phi_4^0\rangle = \frac{1}{2}(|1212\rangle - |1221\rangle - |2112\rangle + |2121\rangle), \tag{3}$$

$$|\phi_4^1\rangle = \frac{1}{\sqrt{12}}(-2|1122\rangle + |1212\rangle + |1221\rangle + |2112\rangle + |2121\rangle - 2|2211\rangle, \tag{4}$$

with the associated potential energies (assuming that the positions are ordered as $x_1 < x_2 < x_3 < x_4$)

$$V|\phi_4^0\rangle = \left[\frac{3}{8}g^2(x_4 - x_3) + \frac{3}{8}g^2(x_2 - x_1)\right]|\phi_4^0\rangle, \tag{5}$$

$$V|\phi_4^1\rangle = \left[g^2\left(\frac{x_4 + x_3}{2} - \frac{x_2 + x_1}{2}\right) - \frac{1}{8}g^2(x_4 - x_3) - \frac{1}{8}g^2(x_2 - x_1)\right]|\phi_4^1\rangle. \tag{6}$$

Evidently, (5) allows asymptotic SU(2) baryons, whereas (6) confines all four quarks. Note that if the ordering of the coordinates changes, then the allowed quark color configurations change accordingly; i.e., the "links" between the particles switch. This is precisely the quark-exchange model [2]. To know whether a force is acting between two given quarks, one must already specify the coordinates of all quarks and the overall color configuration. Since this work deals mainly with the low-density regime, these clusters of two and four quarks will be the only ones included in specific calculations. Such a treatment is exact for the second virial coefficient of the baryon gas, but not for higher coefficients, which contain contributions from interactions between more than two baryons at a time.

However, in general, the possible color configurations in a $2n$-quark system can be represented diagrammatically in the following way: Draw all possible distinct ways of connecting the $2n$ particles pairwise with gluon strings. Two graphs are distinct if there exists a region of space covered by a different number of strings in the two configurations (thus, in the four-quark case, there are only two, not three distinct graphs). The potential energy associated with a graph can now be easily read off by noting that m overlapping strings are associated with an energy density [13]

$$\epsilon_m = \frac{g^2}{8}m(m+2). \tag{7}$$

III. BARYON GAS OF SU(2)-QCD_{1+1}

The effective potential active in two- and four-quark clusters presented above can now be used to derive properties of the nonrelativistic baryon gas. In order for the gas to remain nonrelativistic, $g \ll m$ and $T \ll m$ must be assumed (T denotes the temperature in the system). Furthermore, in order to render the effects of clusters containing more than four quarks negligible, a low baryon density is necessary. In the regime outlined thus, quarks will pair to form SU(2) baryons due to the linear Coulomb interaction, and the baryons will interact via the four-quark quark-exchange potential.

Low density in this context therefore means the fol-

[1]Here, g is the coupling constant appearing in the QCD Lagrangian.

lowing: The probability of finding two further baryons within the interaction radius of a given baryon must be small; that is, $(2d\rho)^2 \ll 1$, where d measures the typical size of a baryon. The baryon size d depends on the temperature regime considered:

(i) At high temperatures, where a large number of excited baryon states contributes, the mean kinetic energy associated with the relative motion of the quarks approaches the classical value $\langle E_{\rm kin}\rangle = T/2$. Because of the virial theorem in a linearly bound system, this implies $\frac{3}{8}g^2\langle d\rangle = \langle E_{\rm pot}\rangle = T$, and therefore $\rho \ll 3g^2\beta/16$.

(ii) At low temperatures, d does not approach zero, but the baryon extension in the ground state, $d \approx (g^2 m)^{-1/3}$; thus, $\rho \ll (g^2 m)^{1/3}/2$.

A. Baryon gas in the classical limit

In this section, the methods of classical statistical mechanics are used to calculate the thermodynamics of the baryon gas. Using the classical approximation implies a further constraint on the parameters of the theory: The thermal wavelength $\lambda = \sqrt{2\pi/mT}$ must be much smaller than the mean interquark distance and the interaction scale. These two conditions here mean essentially the same, since the relevant interquark distance is the one within the baryon, which is controlled precisely by the typical interaction distance; the mean distance between quarks belonging to different baryons, given by the inverse density, is much larger. To make sure that the change in the potential within a thermal wavelength is small on the scale of the kinetic energy, one must have $\frac{3}{8}g^2\lambda \ll T/2$, or roughly $2\sqrt{g/m} \ll (T/g)^{3/2}$. Since $g \ll m$ was already assumed at the beginning, this is fulfilled for a large range of temperatures, even for T appreciably below g.

1. *Gibbs free energy*

For technical reasons, it is advantageous to use the canonical constant pressure ensemble for the problem at hand [14]. In this ensemble, the probability density in phase space is defined as

$$\rho(q_1 \ldots, p_{2N}) = \exp\{\beta[G - Pq_{\max} - H(q_1, \ldots, p_{2N})]\}. \tag{8}$$

The number of quarks in the system is taken to be $2N$, $q_{\max}$ defines the spatial extension of the system, and the Gibbs free energy G is given by the normalization constraint

$$\frac{1}{(2N)!}\sum_C \int_{-\infty}^{\infty} d^{2N}p \int_0^{\infty} d^{2N}q\, \rho = 1, \tag{9}$$

where the prefactor takes account of the indistinguishability of the particles and one must sum over all possible clusterings C of the quarks into groups of either two or four. Clusters of a higher number of quarks are neglected in the present low-density calculation, as explained above.

Since the Hamiltonian takes the form

$$H = \sum_{i=1}^{2N} \frac{p_i^2}{2m} + V(q_1, \ldots, q_{2N}), \tag{10}$$

one can, as usual, immediately perform the momentum integrations in (9). Thus one arrives at

$$G = -\frac{1}{\beta}\ln\left[\left(\frac{2m\pi}{\beta}\right)^N Q\right], \tag{11}$$

with the configuration integral

$$Q = \sum_C \int_0^{\infty} dq_{2N} \int_0^{q_{2N}} dq_{2N-1} \cdots \int_0^{q_2} dq_1\, e^{-\beta(Pq_{2N}+V)} \tag{12}$$

$$= \sum_C Q_C, \tag{13}$$

where use has been made of the fact that the coordinate integrations split up into $(2N)!$ identical contributions characterized by a definite ordering of the particles.

Now one must specify the potential energy. Because of the definite ordering of the quarks, it takes the following simple form for a specific configuration C:

$$V = g^2 \sum_{i=1}^{2N} \epsilon_i^C q_i, \tag{14}$$

where the particles are grouped into clusters of two and four, such that

$$\epsilon_{2i}^C = 3/8, \quad \epsilon_{2i-1}^C = -3/8, \quad \text{or} \quad \epsilon_{2i}^{C'} = 3/8, \quad \epsilon_{2i-1}^{C'} = 5/8, \quad \epsilon_{2i-2}^{C'} = -5/8, \quad \epsilon_{2i-3}^{C'} = -3/8 \tag{15}$$

[cf. (5),(6)]. Now one can evaluate the configuration integral for a specific configuration C by using the properties of the Laplace transform. With the substitutions

$$q_i = \frac{x_i}{\beta g^2}, \qquad P = g^2\gamma, \tag{16}$$

one has, for Q_C,

$$Q_C = \frac{1}{(\beta g^2)^{2N}} \int_0^{\infty} dx_{2N}\, e^{-(\gamma+\epsilon_{2N}^C)x_{2N}} \int_0^{x_{2N}} dx_{2N-1}\, e^{-\epsilon_{2N-1}^C x_{2N-1}} \cdots \int_0^{x_2} dx_1\, e^{-\epsilon_1^C x_1}, \tag{17}$$

and thus one recognizes that the outermost integration represents precisely a Laplace transform with new variable $s = \gamma + \epsilon_{2N}^C$ of the rest of the integral expression. Using

$$\mathcal{L}\left\{\int_0^t d\tau\, f(\tau)\right\} = \frac{1}{s}\mathcal{L}\{f(t)\}, \tag{18}$$

one can successively perform the next-to-outermost integrations to arrive at

$$Q_C = \frac{1}{(\beta g^2)^{2N}} \frac{1}{(\gamma+\epsilon_{2N}^C)(\gamma+\epsilon_{2N}^C+\epsilon_{2N-1}^C)\cdots(\gamma+\epsilon_{2N}^C+\cdots+\epsilon_1^C)}. \tag{19}$$

Because of the correlations between the ϵ_i^C [cf. (15)], clusters of two quarks contribute a factor $(\gamma+3/8)\gamma$ in the denominator, whereas clusters of four quarks give a factor $(\gamma+3/8)(\gamma+1)(\gamma+3/8)\gamma$. Thus, if n_C denotes the number of clusters of four quarks in the configuration C, one has

$$Q_C = \frac{1}{(\beta g^2)^{2N}} \left[\frac{1}{(\gamma+3/8)^2(\gamma+1)\gamma}\right]^{n_C} \left[\frac{1}{(\gamma+3/8)\gamma}\right]^{N-2n_C}, \tag{20}$$

independent of the specific ordering of the clusters. Therefore the sum over color configurations simplifies to a sum over the possible n_C, weighted with the number of possibilities of arranging the given clusters. This corresponds to the problem of choosing n_C out of the $(N-2n_C)+n_C$ clusters which are to be clusters of four quarks. Thus one arrives at

$$Q = \sum_{n_C=0}^{\mathrm{int}(N/2)} \binom{N-n_C}{n_C} Q_C \tag{21}$$

$$= \frac{1}{(\beta g^2)^{2N}} \frac{1}{(\gamma+3/8)^N\gamma^N} \sum_{n_C=0}^{\mathrm{int}(N/2)} \binom{N-n_C}{n_C} \left(\frac{\gamma}{\gamma+1}\right)^{n_C}. \tag{22}$$

Neglecting the possibility of grouping four quarks into one cluster corresponds to taking only the term $n_C = 0$. This term is therefore expected to dominate in the limit of vanishing density.

Sums of the form (22) can be evaluated with the method of generating functions. This is carried out in Appendix A and yields, in the limit of large N,

$$Q = \frac{1}{(\beta g^2)^{2N}} \frac{1}{(\gamma+3/8)^N\gamma^N} \left(x+\frac{1}{2}+\sqrt{x+1/4}\right)^{N/2+1} \left(\frac{1}{2x} - \frac{1}{4x\sqrt{x+1/4}}\right), \tag{23}$$

where

$$x = \frac{\gamma}{\gamma+1}. \tag{24}$$

Thus one obtains, neglecting terms of the order $O(1/N)$, for the Gibbs free energy,

$$G = -\frac{N}{\beta}\left[\ln\left(\frac{2m\pi}{\beta^3 g^4(\gamma+3/8)\gamma}\right) + \frac{1}{2}\ln\left(\frac{\gamma}{\gamma+1}+\frac{1}{2}+\sqrt{\frac{\gamma}{\gamma+1}+\frac{1}{4}}\right)\right]. \tag{25}$$

Note that at this stage one can directly verify that for small densities the additional contribution induced by the four-quark clusters (i.e., the second term in the square brackets) becomes negligible.

2. *Discussion of the thermodynamic behavior*

By differentiation, one can now extract the relevant thermodynamic quantities of the classical baryon gas. For the (one-dimensional) volume of the system one obtains

$$V = \left.\frac{\partial G}{\partial P}\right|_T \tag{26}$$

$$= \frac{N}{\beta}\frac{1}{g^2}\left[\frac{1}{\gamma} + \frac{1}{\gamma+3/8} - \frac{1}{2}\frac{1}{(1+\gamma)^2}\frac{\frac{1}{2}+\sqrt{\frac{\gamma}{\gamma+1}+\frac{1}{4}}}{\frac{\gamma}{\gamma+1}+\frac{1}{4}+(\frac{\gamma}{\gamma+1}+\frac{1}{2})\sqrt{\frac{\gamma}{\gamma+1}+\frac{1}{4}}}\right]. \tag{27}$$

Note that the pressure evidently only depends on the combination ρ/β; the physical reason for this will be elaborated upon further below.

Since the calculation presented here is primarily intended to be a low-density approximation to the baryon gas of QCD_{1+1}, the virial expansion of the equation of state is of particular interest. Rearranging (27) to give the density as a function of the pressure, expanding in the latter (note that low pressures are associated with low densities), and inverting this series gives

$$P = \frac{\rho}{\beta}\left\{1 + \frac{5}{3}\frac{\rho}{g^2\beta} + \frac{2}{3}\left(\frac{\rho}{g^2\beta}\right)^2 - \frac{242}{27}\left(\frac{\rho}{g^2\beta}\right)^3 + O\left[\left(\frac{\rho}{g^2\beta}\right)^4\right]\right\}. \tag{28}$$

The leading term describes an ideal gas of baryons; the first correction, i.e., the second virial coefficient, is an exact result for the classical limit of QCD_{1+1}, since the neglected contributions from clusters of more than two baryons appear in the pressure only at order ρ^3 or higher. The higher-order terms in (28) thus would experience corrections in an exact treatment encompassing all effective interactions induced by QCD_{1+1}. It is to be expected that these corrections are negative, since the additional interactions are of attractive character; the repelling effect of the baryon extension on the other hand is already fully accounted for in the present treatment. The equation of state contained in (27) is therefore expected to be an upper limit for the exact equation of state.

The equation of state implicit in (27) is illustrated in Fig. 1. Already here one can observe how the inclusion of four-quark clusters has lowered the curve with respect to the case where only extended, but otherwise noninteracting baryons are included. Note that in the lower curve, the slope at $\rho = 0$, given by the second virial coefficient, is already exact; including larger clusters merely modifies higher derivatives. On the other hand, the curves converge again in the high-density limit to the value corresponding to an ideal quark gas. This behavior is clear as long as one limits the size of the included clusters as one lets the density grow to infinity: Because the string tensions occurring in the system are then bounded, adding quarks to a given volume at constant temperature leaves the potential energy essentially unchanged, until it becomes negligible compared with the rising kinetic energy. On the other hand, it must be stressed at this point that there is no *a priori* reason why this behavior should persist in an exact calculation, summing up all clusters with an arbitrary number of quarks and then considering the limit $\rho \to \infty$. Of course one expects the ideal quark gas to result also in the full theory, with the plasmon contribution giving the first nontrivial term in a high-density expansion; however, this must be verified by an explicit calculation.

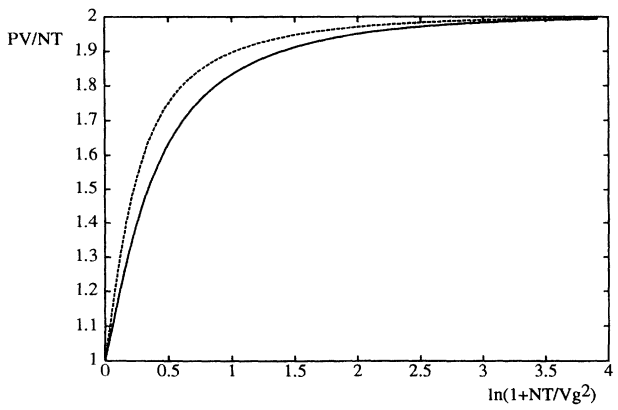

FIG. 1. Equation of state of the nonrelativistic baryon gas in the classical limit. Dashed curve, Only two-quark clusters included; solid curve, two- and four-quark clusters allowed.

Returning in particular to the second virial coefficient, one can already observe the competing effects of the baryon extension and the attractive interaction furnished by the four-quark clusters. Neglecting the latter gives a value of $8/3g^2\beta$ instead of $5/3g^2\beta$ for the second virial coefficient, which is exactly the value expected from a van der Waals equation of state for extended, but otherwise noninteracting objects,

$$P(V - Nd) = N/\beta, \tag{29}$$

in which d is the extension of the particles. The second virial coefficient of this equation of state is simply d; on the other hand, the mean extension of a baryon is just $d = 8/3g^2\beta$ (cf. the estimates given at the beginning of Sec. III). The additional baryon-baryon interaction then lowers this value to the exact one, but is not strong enough to change its sign. Note furthermore that this statement is independent of temperature, as opposed to the usual van der Waals equation of state in three space dimensions, in which particle extension and attractive interaction scale differently with temperature. This is again a manifestation of the already mentioned, and still to be discussed, property that the equation of state depends only on the combination ρ/β.

Apart from the mechanical response of the baryon gas, the thermal behavior is of interest. A very simple form is taken by the thermal expansion coefficient, since the volume of the system is proportional to temperature [cf. (27)]:

$$\alpha_P = \frac{1}{V}\left.\frac{\partial V}{\partial T}\right|_P = \frac{1}{T}. \tag{30}$$

The gas therefore expands exactly as an ideal gas with temperature. For the specific heat one first needs the entropy,

$$S = -\left.\frac{\partial G}{\partial T}\right|_P = -\beta G + 3N. \tag{31}$$

At constant pressure, also the specific heat is very simple:[2]

$$c_P = T \left.\frac{\partial S}{\partial T}\right|_P = 3N. \tag{32}$$

At constant volume, on the other hand, the specific heat becomes complicated. For low densities, one can expand the entropy in powers of the pressure and insert the virial expansion (28). Again taking the derivative with respect to temperature yields

$$c_V = T \left.\frac{\partial S}{\partial T}\right|_V = N\left\{2 - \frac{10}{3}\frac{\rho}{g^2\beta} - 2\left(\frac{\rho}{g^2\beta}\right)^2 + \frac{986}{27}\left(\frac{\rho}{g^2\beta}\right)^3 + O\left[\left(\frac{\rho}{g^2\beta}\right)^4\right]\right\}, \tag{33}$$

where again only the leading and next-to-leading terms are not modified by including larger quark clusters. The leading term is easily understood: The center-of-mass motion of each baryon gives a contribution of 1/2, and its internal kinetic energy likewise. Since, according to the virial theorem, twice as much potential as kinetic energy is associated with the internal motion, an additional contribution of magnitude 1 results. In next-to-leading order, the extension of the baryons again dominates the attractive interaction and leads to the real baryon gas heating up more quickly than the gas of free baryons when the volume is held fixed.

Already in several instances above a trivial scaling of certain thermodynamic quantities with temperature has been exhibited, such as the dependence of the equation of state only on ρ/β or the remarkably simple behavior of α_P and c_P. The physical reason for this is the following: In one space dimension, pressure is not distinct from a constant force, as produced by a linear potential. These two concepts are to a certain extent interchangeable. This becomes especially clear in Eq. (17), where pressure and string tension enter in the same way into the configuration integral, enabling one to extract the temperature as a simple scale of the integration variables. Consider furthermore, e.g., c_P. Here one would argue at low densities that the value $3N$ is composed of the $2N$ which must be invested into the internal energy of the system, and of the mechanical work performed by N baryons. However, one could also interpret the force between the quarks in the baryon as an additional pressure and regard the whole system as a system of $2N$ free quarks (at high densities, this becomes the more natural point of view). Then c_P is composed of a contribution $\frac{1}{2}(2N)$ to the internal energy of the quarks, and of the mechanical work performed against $2N$ particles. The two points of view differ only in whether one interprets the work performed by the quarks against the quark-quark potential as an internal energy or as mechanical work against an external pressure. This interchanging of the concepts also makes plausible why in the second virial coefficient the contributions stemming from the baryon extension, which effectively raises the pressure, on the one hand, and from the baryon-baryon interaction on the other hand must scale in the same way.

One can also express this connection in a complementary manner: Since constant force and pressure are interchangeable effects, the length scales determined by these, i.e., the typical interaction radii of the baryons and the inverse density, respectively, must scale with temperature in the same way. This means that, as long as no further external length scale is introduced, i.e., as long as one is working at constant pressure, a temperature change merely effects a rescaling of the system. This becomes especially clear in the virial theorem for the whole system,[3]

$$2\frac{N}{\beta} = PV + \langle E_{\rm pot}\rangle. \tag{34}$$

Under a scale transformation the two terms on the right-hand side behave linearly in the scale (this is true for arbitrary piecewise linear potentials); therefore, as long as one holds P constant, the rescaling is equivalent to a simple change of the temperature. That is why the response functions at constant pressure become so simple. Ultimately, it is also the reason why the constant pressure ensemble is particularly well suited for the problem at hand. In contrast, if one works at constant volume, an additional length scale is introduced: Heating the system up leads to an increase in the external pressure, while the string tensions remain constant. Thus inverse density and typical baryonic radii scale differently and thermodynamics becomes sensitive to the strength of the interaction, as visible, e.g., in c_V. Note that also a quantum mechanical treatment introduces an additional length scale; this will manifest itself below in a more complicated behavior of the second virial coefficient.

These scaling properties are exhibited also in the following amusing observation: The one-dimensional baryon gas does exhibit the Joule effect, where one achieves the cooling of a gas through free expansion, since

[2]Below, it will become clear that these two results for α_P and c_P remain valid for full QCD_{1+1} in the classical nonrelativistic limit.

[3]A system bound by a quark-exchange-type linear interaction exhibits the same virial theorem as a system bound by a simple linear potential. This is due to the fact that the step functions appearing in the quark-exchange potential introduce no new length scales; the virial theorem on the other hand is simply a manifestation of the scaling properties of the system [2].

$$\left.\frac{\partial T}{\partial V}\right|_U = -\left.\frac{\partial U}{\partial V}\right|_T \left(\left.\frac{\partial U}{\partial T}\right|_V\right)^{-1} \tag{35}$$

and

$$\left.\frac{\partial U}{\partial V}\right|_T = \left.\frac{\partial}{\partial V}(G+TS-PV)\right|_T = -\left.\frac{\partial}{\partial V}(PV)\right|_T \neq 0. \tag{36}$$

However, it does not exhibit the Joule-Thompson effect, where the cooling (or heating) is achieved by letting the gas escape through a valve at constant pressure:

$$\left.\frac{\partial T}{\partial P}\right|_H = -\left.\frac{\partial H}{\partial P}\right|_T \left(\left.\frac{\partial H}{\partial T}\right|_P\right)^{-1} = \frac{1}{c_P}(TV\alpha_P - V) = 0. \tag{37}$$

Since the Joule-Thompson effect in general is the more effective method to cool a gas [15], the usefulness of the baryon gas of QCD_{1+1} as a cooling substance must be regarded as limited.

Note that the arguments above remain valid when all effective interactions induced by QCD_{1+1} are included, since these additional potentials are all linear. One can indeed verify by following the calculation of G that any added linear interaction does not change the simple dependence of the Gibbs free energy on the temperature; only the dependence on pressure is nontrivial. This becomes especially clear in Eqs. (14) and (19). An arbitrary piecewise linear potential can be expressed by a set of coefficients ϵ_i^C. Thus the results for α_P and c_P become exact results for the classical nonrelativistic limit of QCD_{1+1}, valid for all densities. Only in relations implying a fixed external length scale do modifications come about due to the effective interactions neglected here.

B. Baryon-baryon scattering

Beyond the classical treatment performed above, one can derive the second virial coefficient of the quantum system from a calculation of the S matrix for baryon-baryon scattering. Of course the S matrix contains considerably more information than the one thermodynamic function to be extracted here [2]. Thus the calculation to be performed below may be useful also in a wider context, such as in a study of the signatures of quark substructure in a few-hadron system. Such questions, however, will not be addressed further at this point. The method used here is the wave function matching technique described in [2]. It makes use of the fact that for a given ordering of the quark coordinates the Schrödinger equation is trivial to solve and the nontrivial quark-exchange processes only take place on a submanifold of configuration space, the rearrangement surface. The scattering problem can be reduced to a system of equations on this surface, thus making possible the exact solution of a four-body problem.

1. Symmetries of the wave function

Which of the four quarks participating in a baryon-baryon scattering process are coupled through linear potentials depends on the ordering of the coordinates. It suffices, however, to know the wave function for a specific ordering (in the following, $x_1 \leq x_2 \leq x_3 \leq x_4$ is chosen) because of the symmetry properties under the exchange of particles. These symmetries induce boundary conditions at the edges of the sector of configuration space considered. Let the state of the system be represented as a linear combination of the color configurations defined in (4),

$$|\psi\rangle = \int dx_1 dx_2 dx_3 dx_4 \, (\psi_0 |\phi_4^0\rangle + \psi_1 |\phi_4^1\rangle). \tag{38}$$

Starting from $x_1 \leq x_2 \leq x_3 \leq x_4$ one now obtains the boundary conditions by considering the exchange of adjacent quarks. If one exchanges in (38) the variables $x_1 \leftrightarrow x_2$ or $x_3 \leftrightarrow x_4$, respectively, then anticommutation of the relevant quark creation operators shows that $|\phi_4^0\rangle$ remains unchanged, whereas $|\phi_4^1\rangle$ picks up a minus sign (in the sectors reached thus $|\phi_4^0\rangle$ and $|\phi_4^1\rangle$ are still the allowed color configurations). Therefore ψ_0 is symmetric and ψ_1 is antisymmetric under the exchanges $x_1 \leftrightarrow x_2$ or $x_3 \leftrightarrow x_4$.

More interesting is the exchange $x_2 \leftrightarrow x_3$. Here, one reaches a sector of configuration space with a new set of allowed color configurations, which can be expressed in terms of the old ones as

$$\begin{aligned} |\tilde{\phi}_4^0\rangle &= \frac{1}{2}|\phi_4^0\rangle, -\frac{\sqrt{3}}{2}|\phi_4^1\rangle, \\ |\tilde{\phi}_4^1\rangle &= -\frac{\sqrt{3}}{2}|\phi_4^0\rangle - \frac{1}{2}|\phi_4^1\rangle. \end{aligned} \tag{39}$$

In order to give the boundary conditions on the rearrangement surface, it is useful to decompose the state of the system in a different way:

$$\begin{aligned} |\psi\rangle = \int dx_1 dx_2 dx_3 dx_4 \, [&\psi_S(|\phi_4^0\rangle - |\tilde{\phi}_4^0\rangle) \\ &+\psi_A(|\phi_4^0\rangle + |\tilde{\phi}_4^0\rangle)]. \end{aligned} \tag{40}$$

Such a decomposition is always possible due to the relations (39). If one now exchanges $x_2 \leftrightarrow x_3$, anticommutation of the corresponding quark operators shows that $|\phi_4^0\rangle$ changes into $-|\tilde{\phi}_4^0\rangle$, and conversely $|\tilde{\phi}_4^0\rangle$ into $-|\phi_4^0\rangle$. Therefore ψ_S is symmetric under $x_2 \leftrightarrow x_3$, whereas ψ_A is antisymmetric. Translating this back to the original ψ_0 and ψ_1,

$$\begin{pmatrix} \psi_0 \\ \psi_1 \end{pmatrix} = \begin{pmatrix} \frac{1}{2} & \frac{3}{2} \\ \frac{\sqrt{3}}{2} & -\frac{\sqrt{3}}{2} \end{pmatrix} \begin{pmatrix} \psi_S \\ \psi_A \end{pmatrix}, \tag{41}$$

the following boundary conditions on the rearrangement surface $x_2 = x_3$ result:

$$\left.\begin{aligned} \psi_0 &= \tfrac{1}{2}\psi_S \\ \psi_1 &= \tfrac{\sqrt{3}}{2}\psi_S \end{aligned}\right\} \Rightarrow \frac{\psi_1}{\psi_0} = \sqrt{3}, \tag{42}$$

$$\left.\begin{aligned}\partial_n\psi_0 &= \tfrac{3}{2}\partial_n\psi_A \\ \partial_n\psi_1 &= -\tfrac{\sqrt{3}}{2}\partial_n\psi_A\end{aligned}\right\} \Rightarrow \frac{\partial_n\psi_1}{\partial_n\psi_0} = -\frac{\sqrt{3}}{3}, \tag{43}$$

where ∂_n denotes the normal derivative on this surface.

2. Formulation of the scattering problem

For the description of the scattering problem, the following coordinates are useful:

$$R_0 = \frac{1}{2}(x_4 + x_3 + x_2 + x_1), \tag{44}$$

$$R = \frac{1}{2}(x_4 + x_3 - x_2 - x_1), \tag{45}$$

$$r_1 = \frac{1}{\sqrt{2}}(x_2 - x_1), \tag{46}$$

$$r_2 = \frac{1}{\sqrt{2}}(x_4 - x_3). \tag{47}$$

In these coordinates, $x_1 \le x_2 \le x_3 \le x_4$ means (cf. also Fig. 2)

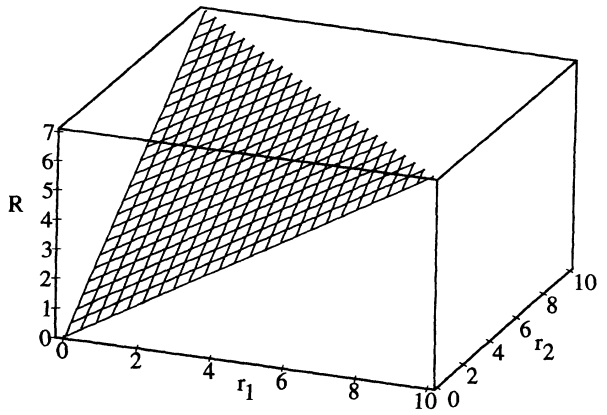

FIG. 2. The rearrangement surface.

$$r_1 \ge 0, \qquad r_2 \ge 0, \qquad R \ge \frac{1}{\sqrt{2}}(r_1 + r_2). \tag{48}$$

The equations of motion in this sector are obtained by projection of $H|\psi\rangle$ [cf. (38)] with $\langle\phi_4^0|$ and $\langle\phi_4^1|$; they read

$$\left[-\frac{1}{2m}\left(\frac{\partial^2}{\partial R^2} + \frac{\partial^2}{\partial r_1^2} + \frac{\partial^2}{\partial r_2^2}\right) + \frac{3\sqrt{2}}{8}g^2(r_1 + r_2)\right]\psi_0 = E\psi_0, \tag{49}$$

$$\left[-\frac{1}{2m}\left(\frac{\partial^2}{\partial R^2} + \frac{\partial^2}{\partial r_1^2} + \frac{\partial^2}{\partial r_2^2}\right) + g^2R - \frac{\sqrt{2}}{8}g^2(r_1 + r_2)\right]\psi_1 = E\psi_1, \tag{50}$$

where the motion in the center-of-mass coordinate R_0 has already been separated off. The boundary conditions now read

$$\text{for } r_1 = 0: \quad \partial_n\psi_0 = 0, \ \psi_1 = 0 \quad \text{with } \partial_n = \partial/\partial r_1; \tag{51}$$

$$\text{for } r_2 = 0: \quad \partial_n\psi_0 = 0, \ \psi_1 = 0 \quad \text{with } \partial_n = \partial/\partial r_2; \tag{52}$$

$$\text{for } R = (r_1 + r_2)/\sqrt{2}: \quad \psi_1/\psi_0 = \sqrt{3}, \quad (\partial_n\psi_1)/(\partial_n\psi_0) = -\sqrt{3}/3$$

$$\text{with } \partial_n = -(1/\sqrt{2})\partial/\partial R + (1/2)\partial/\partial r_1 + (1/2)\partial/\partial r_2; \tag{53}$$

and for asymptotic distances $R \to \infty$ of the baryons,

$$\psi_0^{mm'} \longrightarrow \phi_m(r_1)\phi_{m'}(r_2)e^{-ik_{mm'}R} - \sum_{n,n'} S_{nn'mm'}\phi_n(r_1)\phi_{n'}(r_2)e^{ik_{nn'}R}, \tag{54}$$

$$\psi_1^{mm'} \longrightarrow 0, \tag{55}$$

where the S matrix $S_{nn'mm'}$ has been introduced; m and m' denote the excitation quantum numbers of the incoming baryons, and the functions ϕ_m are the corresponding wave functions, i.e., those solutions of

$$\left[-\frac{1}{2m}\frac{d^2}{dr^2} + \frac{3\sqrt{2}}{8}g^2r\right]\phi_m(r) = \epsilon_m\phi_m(r), \tag{56}$$

which are symmetric at $r = 0$, given explicitly by Airy functions. The relative momenta $k_{mm'}$ are then determined by the chosen total energy E and the internal energies of the baryons:

$$k_{mm'} = \sqrt{2m(E - \epsilon_m - \epsilon_{m'})}. \tag{57}$$

3. Reduction to the rearrangement surface

In order to reduce the problem to the rearrangement surface, one introduces the following functions:

$$\phi^{\pm}_{mm'} = \phi_m(r_1)\phi_{m'}(r_2)e^{\pm ik_{mm'}R}, \tag{58}$$

with the definitions from (56) and (57). For the case $k^2_{mm'} < 0$ the definitions are extended such that the choice of sign of $\mathrm{Im}\, k_{mm'}$ gives exponential decay of $\phi^{\pm}_{mm'}$ for large R. Furthermore one introduces

$$f_{mm'} = f_m(r_1) f_{m'}(r_2) \mathrm{Ai}\left((2mg^2)^{1/3} \left(R - \frac{E - \tilde{\epsilon}_m - \tilde{\epsilon}_{m'}}{g^2} \right) \right). \tag{59}$$

Here the f_m are those solutions of

$$\left[-\frac{1}{2m}\frac{d^2}{dr^2} - \frac{\sqrt{2}}{8} g^2 r \right] f_m(r) = \tilde{\epsilon}_m f_m(r), \tag{60}$$

which are antisymmetric at $r = 0$, again given explicitly by Airy functions. Note that here also the irregular solutions Bi (cf. [16]) are acceptable. The functions f_m are not normalizable on their own, but the complete function $f_{mm'}$ is. However, in the following, the norm of $f_{mm'}$ will be irrelevant.

The functions $\phi^{\pm}_{mm'}$ and $f_{mm'}$ are solutions of the equations of motion (49) and (50), respectively. Furthermore, they fulfill the boundary respective conditions (51) and (52) for the wave functions ψ_0 and ψ_1. Only the constraints on the rearrangement surface (53) are not fulfilled. However, one can now apply Green's theorem to the sector I of configuration space specified in (48) in order to extract relations between the different functions on the rearrangement surface. This can be seen for instance in the case of $\phi^+_{ll'}$ and the wave function $\psi_0^{mm'}$:

$$\begin{aligned} 0 &= \int_I dR\, dr_1 dr_2 \, (\phi^+_{ll'} h \psi_0^{mm'} - \psi_0^{mm'} h \phi^+_{ll'}) \\ &= \int_{\sigma_I} d\sigma \, (\phi^+_{ll'}(-\partial_n)\psi_0^{mm'} - \psi_0^{mm'}(-\partial_n)\phi^+_{ll'}), \end{aligned} \tag{61}$$

where h is the Hamiltonian in the equation of motion (49), to which both $\phi^+_{ll'}$ and $\psi_0^{mm'}$ represent eigenfunctions with eigenvalue E. Now the integral on the surfaces $r_1 = 0$ and $r_2 = 0$ vanishes due to the boundary conditions required for ψ_0, which are, as mentioned above, also fulfilled by $\phi^+_{ll'}$. Only the asymptotic contribution and the one on the rearrangement surface σ_U remain. The asymptotic contribution can be evaluated on a surface with constant, but large R, where the normal derivative is $\partial_n = \partial/\partial R$. Using the orthonormality of the ϕ_l, one obtains

$$\int_{\sigma_R} d\sigma \, (\phi^+_{ll'}(-\partial_n)\psi_0^{mm'} - \psi_0^{mm'}(-\partial_n)\phi^+_{ll'}) = \frac{1}{2}\delta_{lm}\delta_{l'm'} i k_{mm'} \tag{62}$$

(note that the ϕ_l are normalized on $[-\infty, \infty]$). The Green's identity (61) now yields

$$\int_{\sigma_U} d\sigma \, (\phi^+_{ll'}(-\partial_n)\psi_0^{mm'} - \psi_0^{mm'}(-\partial_n)\phi^+_{ll'}) + \frac{i}{2}\delta_{lm}\delta_{l'm'} \mathrm{Re} k_{mm'} = 0, \tag{63}$$

where taking the real part ensures the correct inclusion of closed channels, where the asymptotics give no contribution. In order to simplify the notation, one introduces the scalar product on the rearrangement surface,

$$\begin{aligned} \int_{\sigma_U} d\sigma \, f \cdot g &= 2 \int_0^\infty dR \int_0^{\sqrt{2}R} dt \, f(R, r_1 = \sqrt{2}R - t, r_2 = t) g(R, r_1 = \sqrt{2}R - t, r_2 = t) \\ &= \langle f, g \rangle, \end{aligned} \tag{64}$$

and thus (63) reads

$$\langle \phi^+_{ll'}, -\partial_n \psi_0^{mm'} \rangle - \langle \psi_0^{mm'}, -\partial_n \phi^+_{ll'} \rangle + \frac{i}{2}\delta_{lm}\delta_{l'm'} \mathrm{Re} k_{mm'} = 0. \tag{65}$$

By a completely analogous treatment, one obtains

$$\langle \phi^-_{ll'}, -\partial_n \psi_0^{mm'} \rangle - \langle \psi_0^{mm'}, -\partial_n \phi^-_{ll'} \rangle + \frac{i}{2} S_{ll'mm'} \mathrm{Re} k_{ll'} = 0, \tag{66}$$

$$\langle f_{ll'}, -\partial_n \psi_1^{mm'} \rangle - \langle \psi_1^{mm'}, -\partial_n f_{ll'} \rangle = 0. \tag{67}$$

Due to the conditions on the rearrangement surface (53) one can rewrite the last relation as

$$\frac{\sqrt{3}}{3} \langle f_{ll'}, -\partial_n \psi_0^{mm'} \rangle = \sqrt{3} \langle \psi_0^{mm'}, -\partial_n f_{ll'} \rangle. \tag{68}$$

Equations (65), (66), and (68) determine the S matrix. Note that on the rearrangement surface wave function and normal derivative are independent functions, since the original equations of motion were second-order differential equations.

4. Reduction to an algebraic problem

In order to be able to solve the equations for the S matrix numerically, one must expand the wave function and the normal derivative in a finite set of functions:

$$\psi_0^{mm'} = \sum_{n,n'} a_{mm'nn'} \chi_{nn'}, \tag{69}$$

$$\partial_n \psi_0^{mm'} = \sum_{n,n'} b_{mm'nn'} \tilde{\chi}_{nn'}. \tag{70}$$

Inserting this into the equations for the S matrix, one obtains the matrix equations

$$\begin{aligned} BU - AV + E &= 0, \\ BW - AX &= 0, \\ AY - BZ &= \tilde{S}, \end{aligned} \tag{71}$$

with the matrices

$$\begin{aligned} A_{(mm')(nn')} &= a_{mm'nn'}, & B_{(mm')(nn')} &= b_{mm'nn'}, \\ U_{(nn')(ll')} &= \langle \tilde{\chi}_{nn'}, \phi^+_{ll'} \rangle, & V_{(nn')(ll')} &= \langle \chi_{nn'}, -\partial_n \phi^+_{ll'} \rangle, \\ W_{(nn')(ll')} &= \frac{\sqrt{3}}{3} \langle \tilde{\chi}_{nn'}, f_{ll'} \rangle, & X_{(nn')(ll')} &= \sqrt{3} \langle \chi_{nn'}, -\partial_n f_{ll'} \rangle, \\ Y_{(nn')(ll')} &= \langle \chi_{nn'}, -\partial_n \phi^-_{ll'} \rangle, & Z_{(nn')(ll')} &= \langle \tilde{\chi}_{nn'}, \phi^-_{ll'} \rangle, \\ E_{(mm')(ll')} &= \frac{1}{2} i \mathrm{Re} k_{ll'} \delta_{lm} \delta_{l'm'}, & \tilde{S}_{(mm')(ll')} &= \frac{1}{2} i \mathrm{Re} k_{ll'} S_{ll'mm'}. \end{aligned} \tag{72}$$

Equations (71) can be solved for A and B and thus one obtains the S matrix:

$$\begin{aligned} \tilde{S} &= AY - BZ, \\ A &= BWX^{-1}, \\ B &= -E(U - WX^{-1}V)^{-1}. \end{aligned} \tag{73}$$

The result of the numerical calculation is illustrated in Fig. 3. Details concerning the used set of functions $\chi_{nn'}$ and $\tilde{\chi}_{nn'}$ can be found in Appendix B. Here, a different choice from the one adopted in [2] seems to be necessary due to the fact that the rearrangement surface is now two dimensional.

Note that the numerical calculation must only be carried out for one set of the parameters m and g^2, since the S matrix at different values of these parameters can be determined via the simple scaling properties of a Schrödinger equation with linear potentials. For the eigenvalues and eigenfunctions of such an equation one has

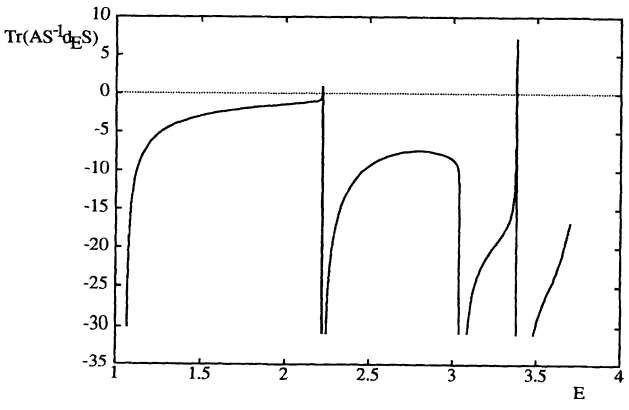

FIG. 3. Result of the numerical calculation, where $m = g = 1$ was chosen. The quantity $\mathrm{Tr}(AS^{-1}\partial_E S)$ plays a crucial role in the determination of the second virial coefficient. In the case of a diagonal S matrix, this would reduce to the sum over energy derivatives of the phase shifts.

$$E_n^{m,g} = \frac{(mg^2)^{2/3} E_n^{m=1,g=1}}{m}, \tag{74}$$

$$\psi_n^{m,g}(x) = (mg^2)^{1/6} \psi_n^{m=1,g=1}[(mg^2)^{1/3} x], \tag{75}$$

where the prefactor of the wave function ensures the proper normalization. Tracking this behavior through the equations for the S matrix, (72) and (73), one obtains

$$S_{m,g}(E) = S_{m=1,g=1}\left(\frac{m}{(mg^2)^{2/3}} E \right). \tag{76}$$

5. *Question of bound states*

When calculating the thermodynamic properties of the baryon gas at low temperatures, it is important to ascertain whether the baryons are capable of forming larger bound states, i.e., nuclei. Bound states between two nuclei would show up as poles in the S matrix at negative energies of relative motion. A search for zeros in the determinant of S^{-1} was unsuccessful in the present model [SU(2) color, one quark flavor]. The absence of two-baryon bound states strongly suggests that there are also no larger nuclei present in the model, since in one space dimension only one nucleon-nucleon bond must be broken for a nucleus to decay. This stands in marked contrast to the three-dimensional case, where in larger nuclei every baryon is bound to several partners, so that much larger binding energies per nucleon than in the deuteron are possible. This effect is very improbable in one space dimension due to the different geometry.

It must be emphasized at this point that the question of bound states depends strongly on the number of quark colors and flavors. While neglecting the color configuration $|\phi_4^1\rangle$ would lead to purely antisymmetric boundary conditions at the rearrangement surface, the inclusion of this additional hidden color configuration weakens the repulsive character of the boundary condition [cf. (53)].

A higher number of quark colors would furnish more color configurations, further strengthening this effect [2]. Thus, at sufficiently high number of colors, a bound state must be expected. Adding additional quark flavors has an even more drastic effect: In the multiflavor case, symmetric boundary conditions (up to the modifications induced by the color configurations) are possible, making the appearance of a bound state very probable.

C. Calculation of the second virial coefficient

From the S matrix, one can determine the second virial coefficient of the baryon gas. Up to order[4] $(e^{\beta\mu})^2$ the pressure is composed of a contribution P_0 associated with the gas of noninteracting baryons with internal excitations, and a contribution from the baryon-baryon interaction, which can be derived from the S matrix [17]:

$$\begin{aligned} P &= P_0 + \frac{1}{\beta} e^{2\beta\mu} \sqrt{\frac{2m}{\pi\beta}} \frac{1}{2\pi i} \int_0^\infty dE\, e^{-\beta E} \mathrm{Tr}\left(A S^{-1} \frac{d}{dE} S \right) \\ &= P_0 + \frac{1}{\beta} e^{2\beta\mu} \sqrt{\frac{2m}{\pi\beta}} \frac{1}{2\pi i} \int_0^\infty dE\, \exp\left(-\beta \frac{(mg^2)^{2/3}}{m} E \right) \mathrm{Tr}\left(A S^{-1}_{m=1,g=1} \frac{d}{dE} S_{m=1,g=1} \right). \end{aligned} \tag{77}$$

Here the symbol A under the trace implies symmetrization in the channels; i.e., instead of $(S^{-1}\partial_E S)_{nn'nn'} + (S^{-1}\partial_E S)_{n'nn'n}$ the trace contains the combination $\frac{1}{2}((S^{-1}\partial_E S)_{nn'nn'} + (S^{-1}\partial_E S)_{nn'n'n} + (S^{-1}\partial_E S)_{n'nnn'} + (S^{-1}\partial_E S)_{n'nn'n})$.

If the baryon gas contained also larger nuclei, then one would obtain already in order $(e^{\beta\mu})^2$ contributions, e.g., from nucleus-nucleus scattering processes. Since these can hardly be treated anymore with the methods presented here, one would have to restrict the validity regime of the calculation to temperatures high enough such that most nuclei are guaranteed to be dissociated.

The interaction contribution can now be extracted from the numeric results for the S matrix, where the scaling in m and g^2 due to (76) only enters as the scale of β, as written out explicitely in (77). Because of the limited amount of included channels, this calculation only makes sense for temperatures well under the highest considered threshold, i.e., roughly $T < 2m/(mg^2)^{2/3}$.

The free contribution P_0 on the other hand results in the following manner: For free baryons with internal degrees of freedom, the contributions of different excited baryon states factorize in the partition function, and the pressure becomes a sum of partial pressures for ideal bosons, where the respective excitation energies simply shift the spectrum:

$$P_0 = -\frac{1}{2\pi\beta} \sum_\alpha \int_{-\infty}^\infty dp\, \ln\left\{ 1 - \exp\left[-\beta\left(\frac{p^2}{4m} + \epsilon_\alpha - \mu \right) \right] \right\} \tag{78}$$

$$= \frac{1}{2\pi\beta} \sum_\alpha e^{-\beta\epsilon_\alpha} \sqrt{\frac{4\pi m}{\beta}} e^{\beta\mu} + \frac{1}{4\pi\beta} \sum_\alpha e^{-2\beta\epsilon_\alpha} \sqrt{\frac{2\pi m}{\beta}} e^{2\beta\mu} + \cdots, \tag{79}$$

with

$$\epsilon_\alpha = -\left(\frac{3}{8}\right)^{2/3} \frac{(mg^2)^{2/3}}{m} c_\alpha, \tag{80}$$

where c_α denotes the zeros of the differentiated Airy function.

As a last step, the expansion in the fugacity $e^{\beta\mu}$ must be translated into the virial expansion. Writing

$$\begin{aligned} P &= \frac{1}{\beta} \sum_{l=1}^\infty b_l e^{l\beta\mu} \stackrel{!}{=} \frac{1}{\beta} \sum_{l=1}^\infty B_l \langle\rho\rangle^l \\ &= \frac{1}{\beta} \sum_{l=1}^\infty B_l \left(\frac{\partial P}{\partial\mu}\Big|_{V,T} \right)^l, \end{aligned} \tag{81}$$

one obtains, by comparing coefficients of the fugacity,

$$B_1 = 1 \qquad \text{and} \qquad B_2 = -\frac{b_2}{b_1^2}, \tag{82}$$

where b_1 and b_2 can be read off from (79) and (77).

Figure 4 shows the result for the second virial coefficient, separated into the free and the interaction parts. Evidently, at low temperatures the attractive effect of bosonic statistics dominates over the pressure increase due to the finite size of the baryons. The second virial coefficient thus rises from negative values towards the classical limit. At temperatures which allow a significant amount of higher baryon excitations in the gas, the numerical result abandons the classical asymptote $\beta g^2 B_2 \to 5/3$, since now channels become important which could not be included anymore in the numerical calculation. From the region around $(mg^2)^{2/3}\beta/m \approx 1$ onwards the numerical result ceases to constitute a good approximation. In the limit $T \to 0$, i.e., $\beta \to \infty$, the integrand in (77) behaves as

[4]Note that the chemical potential μ used here is the Lagrange multiplier associated with baryon, not quark, number.

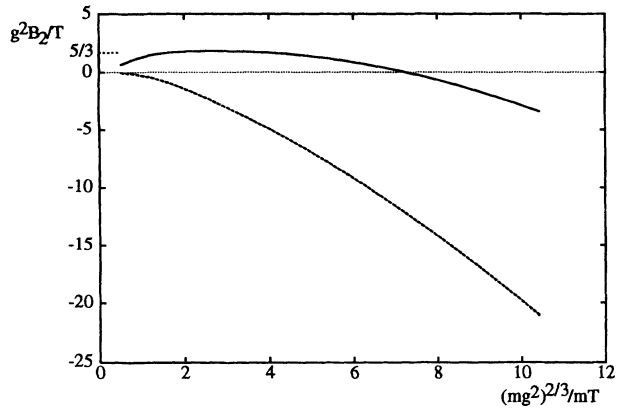

FIG. 4. Second virial coefficient of the nonrelativistic baryon gas. Dashed line, without baryon-baryon interactions; solid line, complete second virial coefficient. The classical limit $\beta g^2 B_2 = 5/3$ is also indicated.

$$\mathrm{Tr}\left(AS^{-1}\frac{d}{dE}S\right)e^{-\beta E} \propto -i\theta(E-2\epsilon_1)\frac{1}{\sqrt{E-2\epsilon_1}}e^{-\beta E} \tag{83}$$

and the contribution to B_2 stemming from the baryon-baryon interaction thus becomes constant in β; the contribution from bosonic statistics on the other hand is proportional to $\sqrt{\beta}$, i.e., it dominates at low temperatures, as mentioned above. Altogether, B_2 behaves as

$$B_2 \sim -\sqrt{\frac{\pi}{8}}\sqrt{\frac{\beta}{m}} + 1.7\frac{1}{(mg^2)^{1/3}} \tag{84}$$

for $\beta \to \infty$.

IV. SUMMARY AND OUTLOOK

Using two complementary approaches, insight has been gained into the behavior of the nonrelativistic baryon gas of QCD_{1+1}. In the classical limit, a fully analytical treatment was possible. Since in this calculation, only configurations were included which cluster up to four quarks, the validity of the calculation is primarily restricted to the low-density regime. However, because of the simple scaling properties exhibited by thermodynamic quantities which do not contain any external length scales, some results proved to remain valid over the entire range of densities. Also, because of the fact that the neglected interactions are attractive, the equation of state derived is expected to constitute an upper bound for the exact equation of state in the classical limit.

On the other hand, the second virial coefficient derived here for the baryon gas is already exact. Supplemented by a quantum mechanical baryon-baryon scattering calculation, a determination of the coefficient for all temperatures was possible. Here, the treatment was simplified by the fact that no larger nuclei form in the one-flavor, two-color case considered; however, in cases where larger nuclei do form, this merely somewhat constrains the temperature regime in which the calculation is valid.

The results derived here should be useful in providing consistency checks for other investigations into the many-body properties of QCD_{1+1}. Unfortunately, it is at this point not possible to perform a detailed comparison with the current Monte Carlo investigations of the ground state [12]; these investigations presently use harmonic confining potentials instead of the linear potentials induced by QCD_{1+1}.

The most serious shortcoming of the calculations presented here is that they are inherently nonrelativistic. Keeping in mind this limitation, it does, however, seem possible to extend the treatment in several ways. On the one hand, it is likely that the classical treatment can be improved to include all effective interactions furnished by QCD_{1+1} in the configuration sum. This would provide the exact equation of state for the whole range of densities, including the interesting transition region between baryon gas and quark plasma. At high densities, contact could be established with perturbation theory [18,19].

On the other hand, the baryon-baryon scattering calculation certainly could be used to gather information about more detailed observables such as correlation functions. Also, to the author's knowledge, there has been no successful calculation of baryon-baryon scattering [for SU(2) color] in the quark-exchange model in three dimensions; the main difference to the meson-meson [2] case lies in the fact that the rearrangement surface is two dimensional instead of one dimensional. Since it was possible to overcome this difficulty in the case considered here, the three-dimensional problem may eventually prove to be tractable. It would be interesting to see whether there are any qualitative differences to the meson-meson case.

In concluding, it would seem useful to connect a scattering calculation with the second virial coefficient also in the classical case [20]. Since in the case at hand a direct analytical determination of the thermodynamical properties was possible, such an approach would have been unnecessarily complicated, especially since it seems to require numerical work. However, in more complicated systems, where no simple evaluation of the partition function is possible, this may be a viable replacement. In general, there should be a deep connection between the density of states and the behavior of the scattering problem under scale transformations [21].

ACKNOWLEDGMENTS

The author is indebted to F. Lenz, S. Lenz, and D. Stoll for fruitful discussions. Generous support by the Institut für theoretische Physik III of the Universität Erlangen-Nürnberg, where most of this work was done, is also acknowledged. This work was financed in part by the Bundesminister für Forschung und Technologie (Germany) and by a MINERVA fellowship.

APPENDIX A: THE EVALUATION OF THE GIBBS FREE ENERGY

Consider for simplicity an even number of baryons $N = 2N'$. Defining the generating function

$$Q(z) = \sum_{n=0}^{\infty}\sum_{k=0}^{n}\binom{2n-k}{k}x^k z^n = \sum_{k=0}^{\infty}\sum_{n=k}^{\infty}\binom{2n-k}{k}x^k z^n \tag{A1}$$

$$= \sum_{k=0}^{\infty}\sum_{n=0}^{\infty}\binom{2n+k}{k}x^k z^{n+k} = \sum_{n=0}^{\infty}\frac{z^n}{(2n)!}\left(\frac{d}{d(xz)}\right)^{2n}\sum_{k=0}^{\infty}(xz)^{2n+k} \tag{A2}$$

$$= \sum_{n=0}^{\infty}\frac{z^n}{(2n)!}\left(\frac{d}{d(xz)}\right)^{2n}\frac{1}{1-xz} = \sum_{n=0}^{\infty}z^n\frac{1}{(1-xz)^{2n+1}} \tag{A3}$$

$$= \frac{1}{1-xz}\left(1-\frac{z}{(1-xz)^2}\right)^{-1} = \frac{1-xz}{(1-xz)^2-z}, \tag{A4}$$

one can extract the N'th Taylor coefficient Q [cf. (22)] via

$$Q = \sum_{k=0}^{N'}\binom{2N'-k}{k}x^k = \frac{1}{2\pi i}\oint\frac{dz}{z^{N'+1}}Q(z). \tag{A5}$$

$Q(z)$ is meromorphic with simple poles, when $(1-xz)^2 = z$, i.e.,

$$z_{1,2} = \frac{1}{x^2}\left(x+\frac{1}{2}\pm\sqrt{x+\frac{1}{4}}\right) > 0 \quad \text{for } x > 0. \tag{A6}$$

Deforming the integration path to infinity, one is left with the residues at the two poles:

$$Q = -\mathrm{res}_{1,2}\left(\frac{Q(z)}{z^{N'+1}}\right) = -\sum_i \lim_{z\to z_i}(z-z_i)\frac{Q(z)}{z^{N'+1}}$$

$$= -\frac{1-\frac{1}{x}(x+\frac{1}{2}+\sqrt{x+\frac{1}{4}})}{2\sqrt{x+\frac{1}{4}}[\frac{1}{x^2}(x+\frac{1}{2}+\sqrt{x+\frac{1}{4}})]^{N'+1}} + \frac{1-\frac{1}{x}(x+\frac{1}{2}-\sqrt{x+\frac{1}{4}})}{2\sqrt{x+\frac{1}{4}}[\frac{1}{x^2}(x+\frac{1}{2}-\sqrt{x+\frac{1}{4}})]^{N'+1}}. \tag{A7}$$

Introducing a common denominator yields

$$Q = \frac{1}{4x\sqrt{x+1/4}}\left[\left(x+\frac{1}{2}-\sqrt{x+1/4}\right)^{N'+1} - \left(x+\frac{1}{2}+\sqrt{x+1/4}\right)^{N'+1}\right]$$
$$+\frac{1}{2x}\left[\left(x+\frac{1}{2}-\sqrt{x+1/4}\right)^{N'+1} + \left(x+\frac{1}{2}+\sqrt{x+1/4}\right)^{N'+1}\right]. \tag{A8}$$

For large N' the second terms in the parentheses dominate, respectively, and (A8) reduces to the result given in Sec. III A 1 (note that $2N' = N$).

APPENDIX B: DETAILS OF THE SCATTERING CALCULATION

In meson-meson scattering calculations [2], the set

$$\chi_{nn'} = \phi^+_{nn'}, \qquad \tilde{\chi}_{nn'} = \partial_n\phi^+_{nn'} \tag{B1}$$

was used to expand the wave function [cf. (58)]. This choice had the advantage of reducing the number of matrix inversions needed. In the case at hand, however, it has the following disadvantages:

(i) The $\phi^+_{nn'}$ and their normal derivatives, respectively, do not constitute an orthonormal set on the rearrangement surface σ_U.

(ii) The $\phi^+_{nn'}$ do not disappear quadratically at the edges of the rearrangement surface. This, however, is a property of the functions $\psi_0^{mm'}$ which are to be expanded: On the surfaces $r_1 = 0$ and $r_2 = 0$ the conditions (51) and (52) hold. Since, on the other hand, on the rearrangement surface itself ψ_0 and ψ_1 are proportional to each other, it follows that at its edge, where it meets the surfaces $r_i = 0$, ψ_0 as well as its derivative in the r_i direction must vanish.

These two missing properties lead to bad convergence and numerical instability in the calculations. Therefore, a different set was used here:

(i) In "radial" direction on the rearrangement surface (i.e., in the direction $r_1 = r_2$) Airy functions with nodes at the origin; this takes account of the property that the system is bound linearly at large R. Since it is *a priori* not clear what effective "inertia" the dynamics of the full system induces for the "motion" on the rearrangement surface, the ansatz contains a freedom in the scaling with R. For this scale, several values were used to test the stability of the calculation.

(ii) Perpendicular to this, i.e., for constant R, an orthogonal set of functions which vanishes quadratically at the edge of the rearrangement surface:

$$\left.\begin{aligned} L_m(x) &= \sin^2 x P_m^{3/2,-1/2}(1-2\sin^2 x) \\ L_{\widetilde{m}}(x) &= \sin^2 x \cos x P_{\widetilde{m}}^{3/2,1/2}(1-2\sin^2 x) \end{aligned}\right\} m,\widetilde{m} \geq 0, \tag{B2}$$

with the Jacobi polynomials $P_m^{jj'}$ [16].

Summing up, the following set of functions was used:

$$\chi_{mm'}(R,t) = \tilde{\chi}_{mm'}(R,t) = N_{mm'}\sqrt{\frac{\pi}{\sqrt{2}R}} L_m(\pi t/\sqrt{2}R)\,\mathrm{Ai}((\mu m g^2)^{1/3}R - c_{m'}). \tag{B3}$$

The $c_{m'}$ are the zeros of the Airy function and μ is the free scale parameter mentioned above. Note that despite of the R-dependent normalization of the L_m, the nodes of the Airy functions at the origin guarantee that the whole function vanishes there.

The functions $\chi_{mm'}$ defined thus are orthogonal with respect to the scalar product on the rearrangement surface (64) and can be normalized with respect to the same, yielding the normalization factor $N_{mm'}$. In the numerical calculations of the matrices (72) the sets were cut off such that $0 \leq m + m' \leq M$, where $M = 3$ was mostly used, and checks of convergence were carried out with $M = 9$; this yields 10×10 or 55×55 matrices, respectively. Using 55 channels rather deteriorated numerical stability; this seems to be due to the fact that the matrices acquire very large or small determinants. For the scale μ the values 1, 3, and 4 were used, where $\mu = 4$ fulfilled criteria such as the unitarity of the S matrix best as energy was increased. Typically, a calculation with ten channels for one fixed value of the total energy took a few hours CPU time on a HP 9000/720 workstation.

[1] *Quark-Gluon Plasma,* edited by R.C. Hwa (World Scientific, Singapore, 1990).
[2] F. Lenz, J.T. Londergan, E.J. Moniz, R. Rosenfelder, M. Stingl, and K. Yazaki, Ann. Phys. (N.Y.) **170**, 65 (1986).
[3] O.W. Greenberg and H.J. Lipkin, Nucl. Phys. **A370**, 349 (1981).
[4] S. Gardner, Phys. Rev. C **42**, 2193 (1990)
[5] C. Alexandrou, T. Karapiperis, and O. Morimatsu, Nucl. Phys. **A518**, 723 (1990).
[6] G. Röpke, D. Blaschke, and H. Schulz, Phys. Lett. B **174**, 5 (1986).
[7] G. Röpke, D. Blaschke, and H. Schulz, Phys. Rev. D **34**, 3499 (1986).
[8] Ch. Barter, D. Blaschke, and H. Voss, Phys. Lett. B **293**, 423 (1992).
[9] C.J. Horowitz, E.J. Moniz, and J.W. Negele, Phys. Rev. D **31**, 1689 (1985).
[10] C.J. Horowitz and J. Piekarewicz, Phys. Rev. C **44**, 2753 (1991).
[11] C.J. Horowitz and J. Piekarewicz, Nucl. Phys. **A536**, 669 (1992).
[12] S. Gardner, C.J. Horowitz, and J. Piekarewicz, Phys. Rev. C **50**, 1137 (1994).
[13] M. Engelhardt and B. Schreiber, Z. Phys. A (to be published).
[14] A. Lenard, J. Math. Phys. **2**, 682 (1961).
[15] L.E. Reichl, *A Modern Course in Statistical Physics* (University of Texas Press, Austin, 1980).
[16] *Handbook of Mathematical Functions,* edited by M. Abramowitz and I.A. Stegun (Dover, New York, 1965).
[17] R. Dashen, S. Ma, and H.J. Bernstein, Phys. Rev. **187**, 345 (1969).
[18] M. Engelhardt, Ph.D. thesis, Erlangen University, 1994.
[19] L.D. McLerran and A. Sen, Phys. Rev. D **32**, 2794 (1985).
[20] R. Dashen and S. Ma, Phys. Rev. A **4**, 700 (1971).
[21] F. Lenz (private communication).